




FFG

 Bundesministerium
Klimaschutz, Umwelt,
Energie, Mobilität,
Innovation und Technologie

IoT Fan

D3.1. Documentation of lab experiments with IoT enabled components of heat pumps

Submitted by:

Christoph Reichl (christoph.reichl@ait.ac.at)

AIT – Austrian Institute of Technology GmbH

Center for Energy

Sustainable Thermal Energy Systems

Giefinggasse 4, A 1210 Wien, Österreich



Project team: Camilla Sandström, Albert Heinrichs, Johannes Krämer, Veronika Wilk

Vienna, December 2021, updated May 2023



Index

1. Introductory Remarks.....	3
2. Introduction	3
3. Heat pump icing testrig	4
3.1. Measurement C+55	6
3.2. Measurement U+55	7
3.3. Measurement U+45	8
3.4. Measurement C+20	9
3.5. Measurement U+20	10
3.6. Measurement U-20	11
3.7. Discussion.....	11
4. Evaporator icing testrig	13
4.1. Fan Control with the Adjustable Power Supply	14
4.2. Data Measurement and Collection	14
4.3. Vibration measurements during defrosting	15
4.4. Vibration measurements during artificial heat exchanger blocking	16
5. Summary	18
6. Acknowledgements	19



1. Introductory Remarks

This is a deliverable of the Austrian project for IEA HPT Annex 56 (Digitalization and IoT for heat pumps). The IEA HPT Annex 56 project explores the opportunities and challenges of connected heat pumps in household applications and industrial environment. There are a variety of new use cases and services for IoT enabled heat pumps. Data can be used for preventive analytics, such as what-if analysis for operation decisions, predictive maintenance, fine-tuning of the operation parameters and benchmarking. Connected heat pumps allow for demand response to reduce peak load and to optimize electricity consumption, e.g., as a function of the electricity price. Digitalization in industry can range from automated equipment, advanced process control systems to connected supply value chains. IoT enabled heat pumps allow for integration in the process control system and into a high-level energy management system, which can be used for overall optimization of the process. IoT is also associated to different important risks and requirements to connectivity, data analysis, privacy and security for a variety of stakeholders. Therefore, this Annex has a broad scope looking at different aspects of digitalization and creates a knowledge base on connected heat pumps. The Annex aims to provide information for heat pump manufacturers, component manufacturers, system integrators and other actors involved in IoT.

This document describes experiments carried out at AIT Austrian Institute of Technology with an IoT ready fan with integrated vibration measurement (WP3 of the Austrian project for IEA HPT Annex 56). The experiments have been setup and performed to gain the necessary time correlated fan vibration and evaporator frosting data to extract a soft sensor (WP4 of the Austrian project for IEA HPT Annex 56). This sensor would be able to correlate the evaporator frosting state to the measured vibrations of the fan. Two setups for measurements are presented.

2. Introduction

Air is forced through the evaporator by a fan situated behind the heat exchanger. As the fan operates some vibrations are present due to the continuous movement. This is normal for all operating fans, but in some cases the fan vibrations, due to different circumstances, can increase to values where the operational performance is affected. Increased vibrations can cause structural damage to the fan bearings and in some cases transmit to adjacent areas. If a malfunction of the fan occurs, it could create a shutdown of the heat pump due to missing airflow through the heat exchanger. Excessive vibrations can also increase noise annoyance to the surroundings. As frost grows unevenly on the heat exchanger disturbances in the airflow can occur. The resulting air pressure loss from the blockage redirects the air flow to less frosted areas and an uneven flow through the fins could affect the fan. The appearance of vibration due to frosting on ASHPs have not been researched in open literature and therefore will be examined here in the report.

Out of these investigations, a soft sensor for evaporator ice detection based on vibration signals recorded by the fan is developed.

Therefore, an initial measuring system was set up based on a test heat pump. This consists of the refrigeration circuit with compressor, the air heat exchanger, and the fan unit, which is equipped with a vibration measuring system, the data of which can be directly imported into the measured value recording. The test heat pump is positioned on a scale in order to be able to determine the total weight of the heat pump and thus also the mass of the attached ice. The extraction of the scale signal is also time dependent. In order to obtain further conclusions about



the ice build-up on the heat exchanger, two video cameras were positioned. They produce an overview image and a detailed image with high magnification optics. The measurement system was set up, successfully tested and measurements were taken.

Initial analyses show transient changes in the vibration signal. However, in order to better delineate the vibration behavior of the heat exchanger - fan unit, measurements without a directly coupled compressor were necessary. For this purpose, a second setup was created, where the air heat exchanger - fan unit was operated with a coolant that is vibration-mechanically decoupled and supplied by an external refrigeration system. The icing characterization was carried out by means of image analysis and balance signal. Here, we present the initial assembly and the related measurements, the new modified setup and the conclusions.

3. Heat pump icing testrig

In the framework of the SilentAirHP project, an experimental heat pump has been designed with the primary focus on acoustic measurements. However, it was found, that icing of the evaporator leads to increasing sound pressure levels and plays an important part in transient heat pump acoustics. In the SilentAirHP project, vibration signals have not been recorded. It was decided later on, to use the existing setup and exchange the fan by a new generation version, which was capable of measuring the vibration of the fan. These signals have been recorded in addition to the weight of the heat pump and the two video streams showing an overview and a detailed part of the evaporator's fin surface (see Figure 1).

The icing measurements (without vibration signal discussed) are in detail described in the papers:

- Ch. Reichl, C. Sandström, F. Hochwallner, F. Linhardt, M. Popovac, J. Emhofer, Frosting in heat pump evaporators part A: Experimental investigation, Applied Thermal Engineering, Volume 199, 2021, 117487, ISSN 1359-4311, <https://doi.org/10.1016/j.applthermaleng.2021.117487>.
(<https://www.sciencedirect.com/science/article/pii/S1359431121009182>)
- M. Popovac, J. Emhofer, Ch. Reichl, Frosting in a heat pump evaporator part B: Numerical analysis, Applied Thermal Engineering, Volume 199, 2021, 117488, ISSN 1359-4311, <https://doi.org/10.1016/j.applthermaleng.2021.117488>.
(<https://www.sciencedirect.com/science/article/pii/S1359431121009200>)

Furthermore, results are explained in detail in the master thesis of Camilla Sandström, which has been performed in a collaboration between KTH Stockholm and AIT Vienna.

- C. Sandström, Frosting and Defrosting on Air Source Heat Pump Evaporators, KTH Industrial Engineering and Management, 2021. [Frosting and Defrosting on Air Source Heat Pump Evaporators \(diva-portal.org\)](https://diva-portal.org/urn:nbn:se:kth:diva-18111)

Here we present data from the vibration sensors. Data is available for several thermal conditions of the climatic chamber. Measurements have been performed with a coated and an untreated evaporator.

Several conditions have been measured and are summarized in Table 1 and 2 stating environmental conditions and temperatures in the evaporator. Vibration data for selected measurements are presented in the sections below.



Measurement	Inlet temperature °C	Inlet r.h. (spec.h.) % (g/kg)	Outlet temperature °C	Outlet r.h. (spec.h.) % (g/kg)	Surface treatment
U+55	5.4 ± 0.1	95.5 ± 1.0 (5.4)	1.7 ± 0.5	90.0 ± 0.5 (3.9)	None
U+45	4.4 ± 0.1	95.0 ± 1.0 (5.0)	0.7 ± 0.2	89.3 ± 0.5 (3.6)	None
U+20	1.8 ± 0.2	91.0 ± 0.5 (4.0)	-1.4 ± 0.2	84.7 ± 0.5 (2.9)	None
U-20	-2.0 ± 0.2	86.5 ± 1.5 (2.4)	-5.2 ± 0.4	80.0 ± 2.0 (2.0)	None
C+55	5.3 ± 0.2	90.5 ± 1.5 (5.1)	0.8 ± 0.2	78.0 ± 2.0 (3.2)	Nano-fluid
C+45	4.4 ± 0.1	90.5 ± 1.5 (4.8)	0.2 ± 0.5	78.5 ± 2.0 (3.1)	Nano-fluid
C+20	1.8 ± 0.1	89.0 ± 0.6 (3.9)	-1.5 ± 0.5	80.0 ± 1.5 (2.7)	Nano-fluid
C-20	-2.1 ± 0.2	85.5 ± 1.2 (2.8)	-5.5 ± 0.5	80.0 ± 2.0 (1.9)	Nano-fluid

Table 1: Environmental conditions up- and downstream of the evaporator

Measurement	T(p ₂) °C	T(p ₄) °C	T ₅ °C	T(p ₁) °C	Compressor speed Hz	Avg. heating power kW
U+55	-4.8 ± 3.4	-7.7 ± 3.4	0.5 ± 5.4	35.8 ± 1.3	66	3.6 ± 0.8
U+45	-5.8 ± 3.2	-8.8 ± 3.2	-0.9 ± 6.0	35.5 ± 1.8	66	3.5 ± 0.8
U+20	-7.1 ± 3.3	-11.7 ± 3.4	-3.0 ± 6.2	36.2 ± 1.5	82	4.0 ± 0.9
U-20	-10.4 ± 3.5	-14.8 ± 3.5	-7.3 ± 7.0	35.2 ± 2.1	82	3.6 ± 0.7
C+55	-4.8 ± 3.3	-8.0 ± 3.5	-0.7 ± 3.8	35.2 ± 1.8	66	3.6 ± 0.6
C+45	-6.4 ± 2.6	-9.5 ± 2.7	-1.8 ± 5.6	35.5 ± 1.1	68	3.6 ± 0.8
C+20	-7.6 ± 2.6	-12.6 ± 2.8	-4.1 ± 6.2	36.3 ± 2.0	86	4.0 ± 0.9
C-20	-9.9 ± 3.3	-14.7 ± 3.4	-7.5 ± 5.8	35.2 ± 2.8	82	3.6 ± 0.7

Table 2: Temperatures in the evaporator and average heating power at the condenser

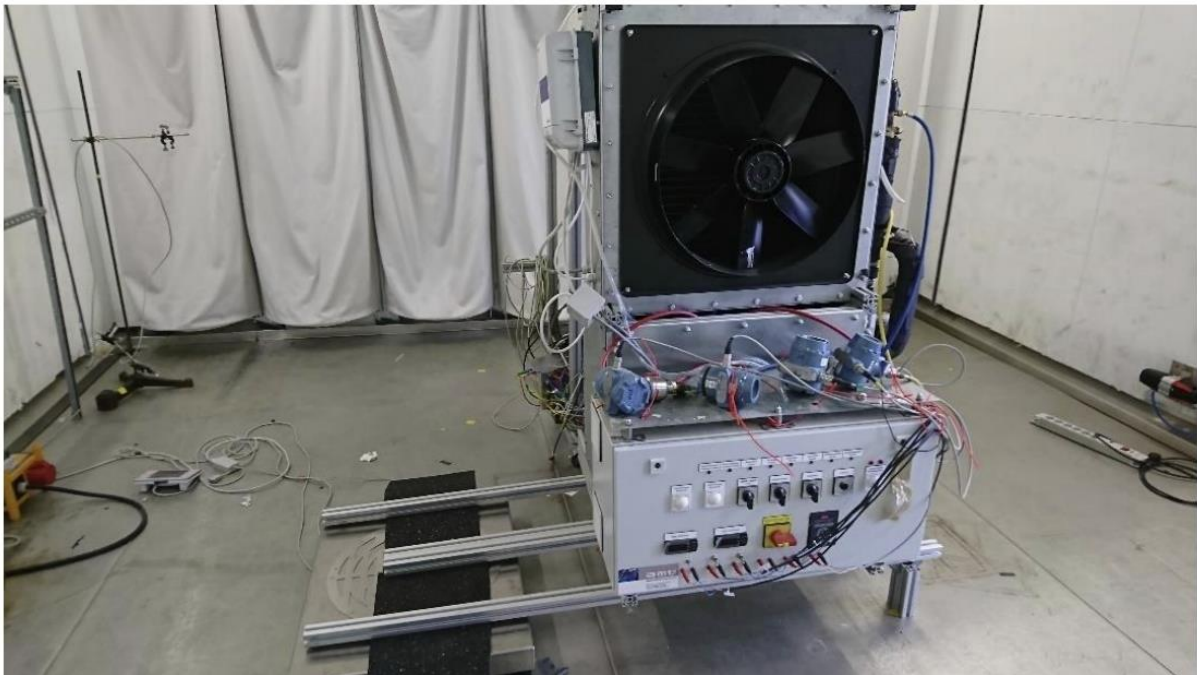


Figure 1: Heat pump mounted on top of a scale placed in the climate chamber.

3.1. Measurement C+55

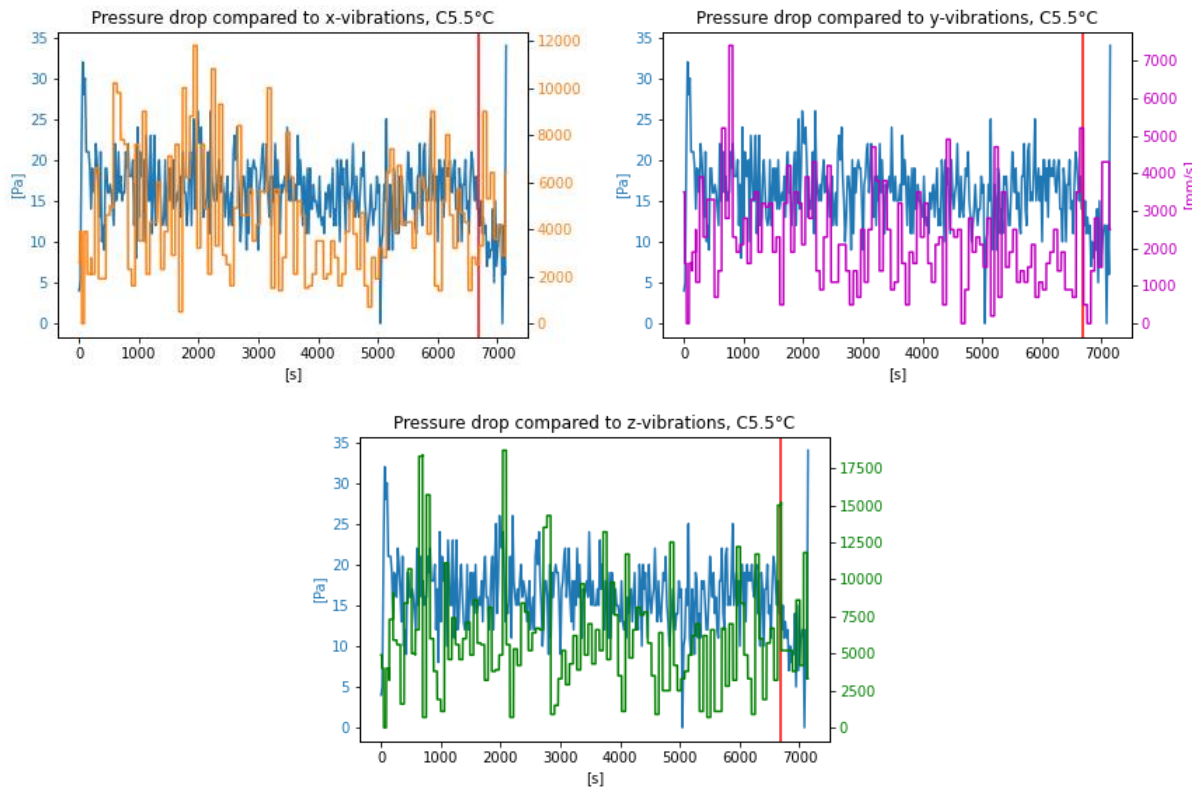


Figure 2: Pressure drop compared to the three components of the fan vibration signal for the coated evaporator at a temperature of 5.5°C in the climatic chamber

3.2. Measurement U+55

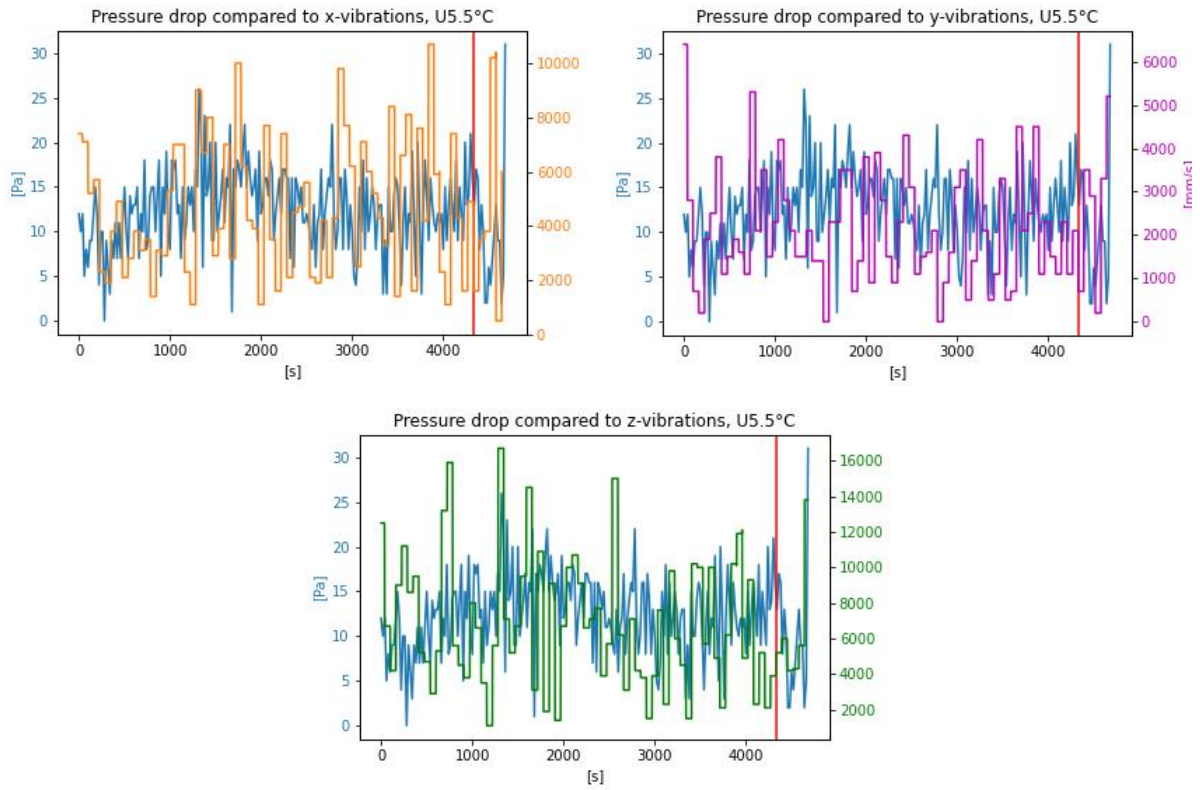


Figure 3: Pressure drop compared to the three components of the fan vibration signal for the untreated evaporator at a temperature of 5.5°C in the climatic chamber

3.3. Measurement U+45

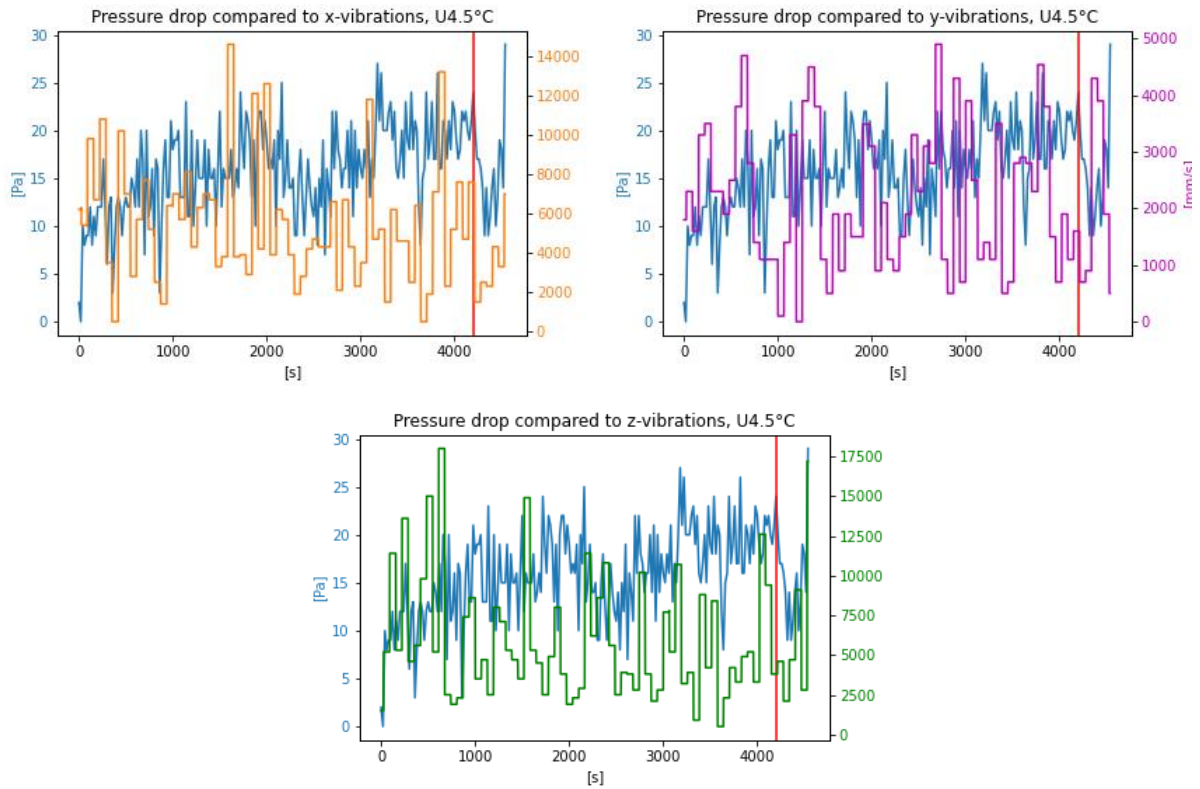


Figure 4: Pressure drop compared to the three components of the fan vibration signal for the untreated evaporator at a temperature of 4.5°C in the climatic chamber

3.4. Measurement C+20

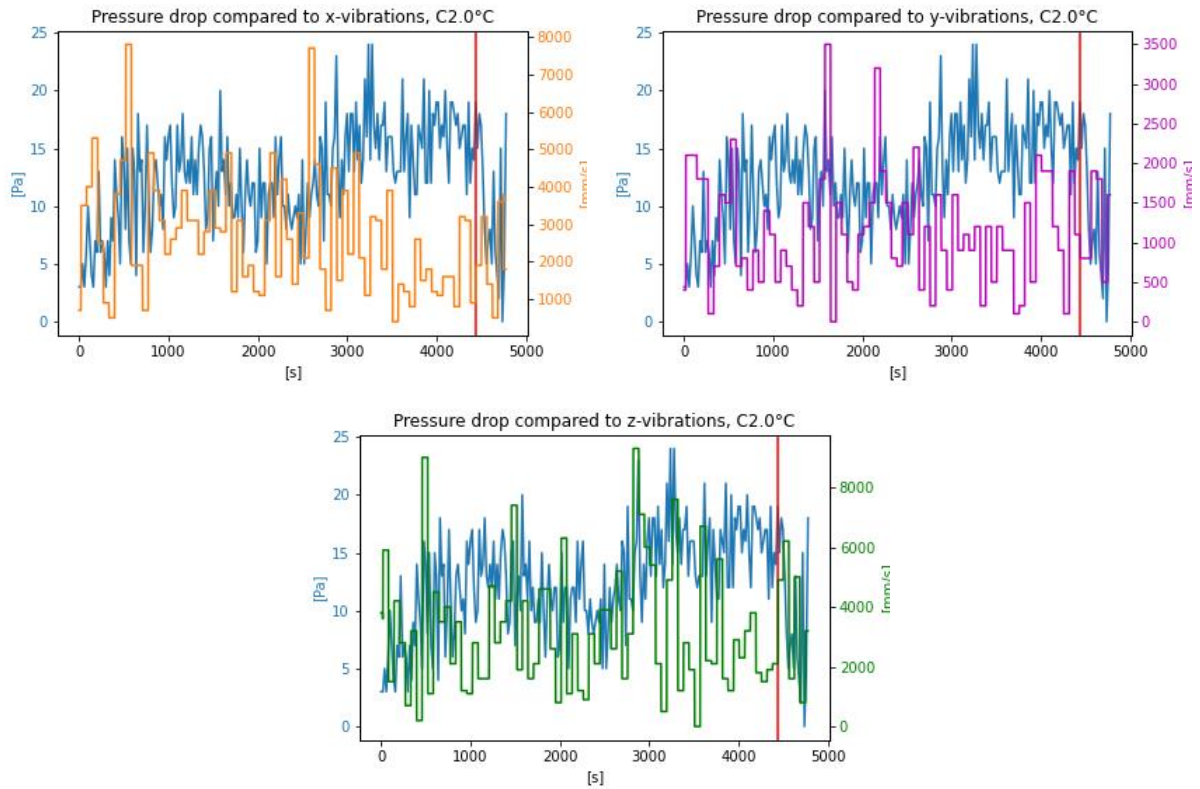


Figure 5: Pressure drop compared to the three components of the fan vibration signal for the coated evaporator at a temperature of 2.0°C in the climatic chamber

3.5. Measurement U+20

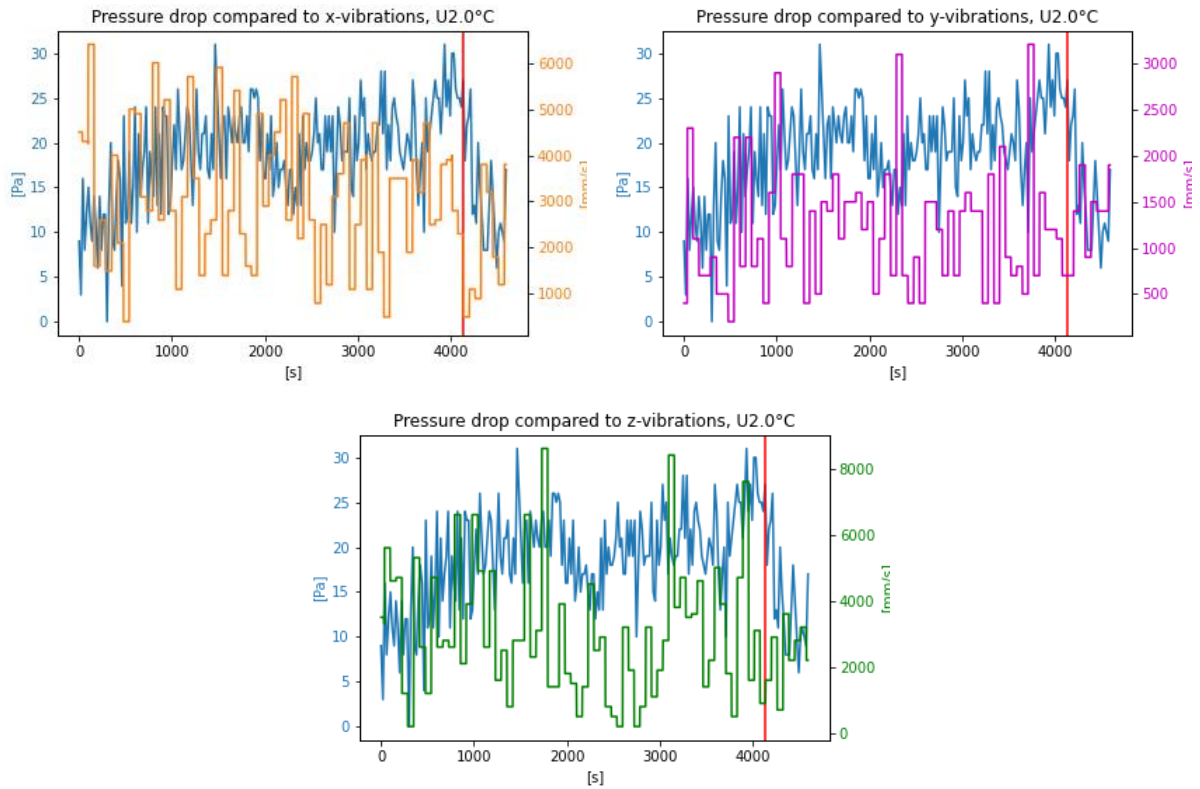


Figure 6: Pressure drop compared to the three components of the fan vibration signal for the untreated evaporator at a temperature of 2.0°C in the climatic chamber

3.6. Measurement U-20

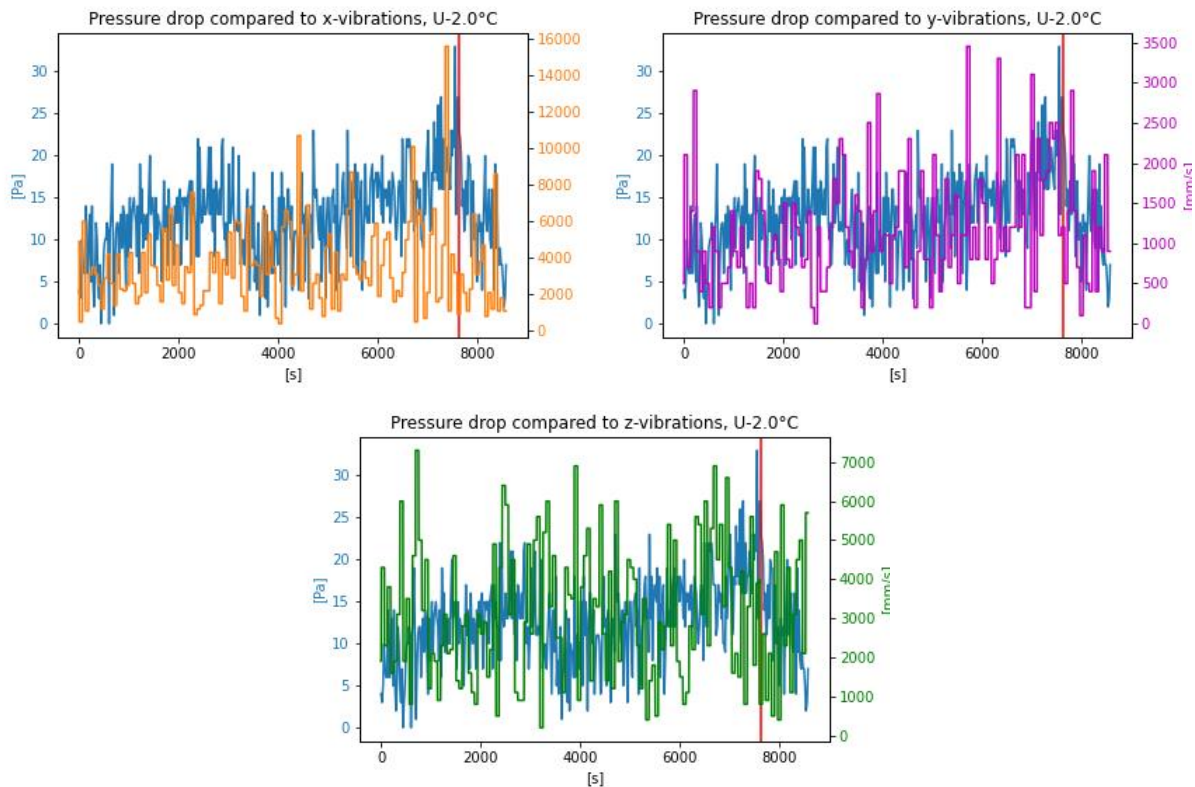


Figure 7: Pressure drop compared to the three components of the fan vibration signal for the untreated evaporator at a temperature of -2.0°C in the climatic chamber

3.7. Discussion

Fan vibrations were measured under frosting conditions by a sensor situated in the fan for vibrations in the x-, y- and z- direction. The measured data was compared to heat pump operational functions to investigate if the frost on the heat exchanger affects the fan vibrations. As seen in seen in Figure 8, presenting the vibrations in measurement U+55, no clear correlation to between the vibrations and frosting can be seen as the vibrations seem random throughout the measurement. The vibration output was obtained for every second, but the value obtained from the sensor was only updated once every minute which can be seen in the figure behavior. The x- and z-axis present similar behavior indicating the vibrations in the rotational plane while the y-axis is along the rotational axis having lower level of vibrations. No correlation was found in any of the measurements.

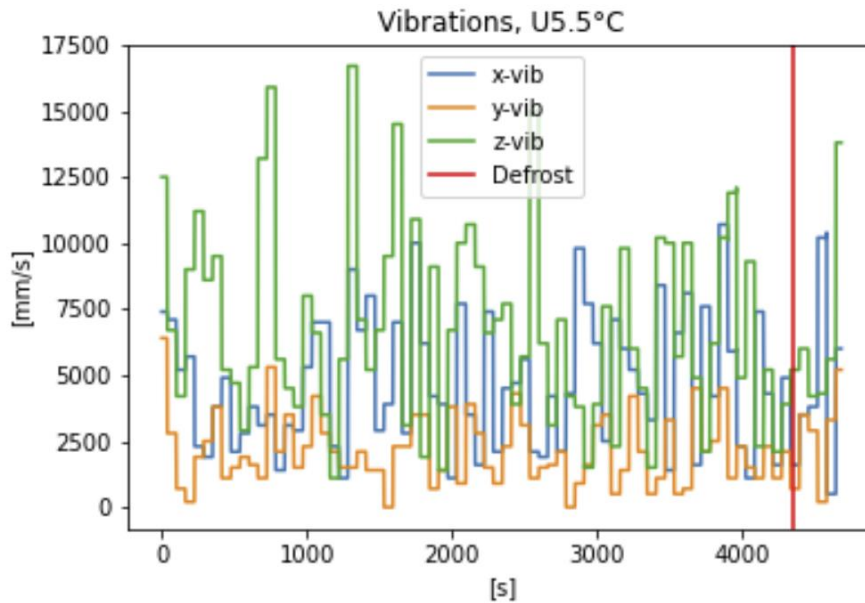


Figure 8: Vibration measurements in x-, y-, and z-axis for measurement U+55

Looking at the mean value of the vibrations from the whole cycle, the vibrations are reduced with lower ambient temperature. The variation in the vibration is still high for all measurements and axis directions. In Table 3 below the mean values and standard deviation for each measurement is displayed. The random behavior of the vibrations led to noisy outputs with high standard deviations. Vibrations were missing from the measurements C+45 and C-20 due to connection problems.

Vibration axis →	x		y		z	
Measurement ↓	Mean	Stdev	Mean	Stdev	Mean	Stdev
C+55	4508	2525	2205	1290	5908	3652
U+55	4647	2522	2133	1298	6711	3592
C+45	-	-	-	-	-	-
U+45	5311	3017	2169	1260	5815	3698
C+20	2626	1524	1127	694	3213	2053
U+20	3050	1506	1211	635	2981	1918
C-20	-	-	-	-	-	-
U-20	3527	2279	1158	716	3128	1739

Table 3: Mean values and standard deviations for vibrations in x-, y-, and z-axis.

No conclusion between the frosting and vibrations can be drawn from the data obtained in this experiment. This experiment indicates that no correlation is present but further research between the correlation of frost, vibrations and ambient temperature must be made. A better resolution in time and vibration value is needed to evaluate the correlation.

4. Evaporator icing testrig

To circumvent some of the problems, which arose during the tests with the SilentAirHP, a new setup was considered removing the compressor as a possible source of vibrations. The disassembled heat pump (dhp) consisting only of the evaporator is connected via isolated tubing to the cold-water reservoir. The pump responsible for the mass transport is situated on the warm water side. The dhp stands slightly elevated (due to tubing on its bottom) on a scale. The dhp is secured on 3 points against sliding off the scale using vertical aluminum profiles. Mounted on the dhp is a fan. The fan is controlled through the voltage supplied by an adjustable power supply (see Figures 9 and 10).

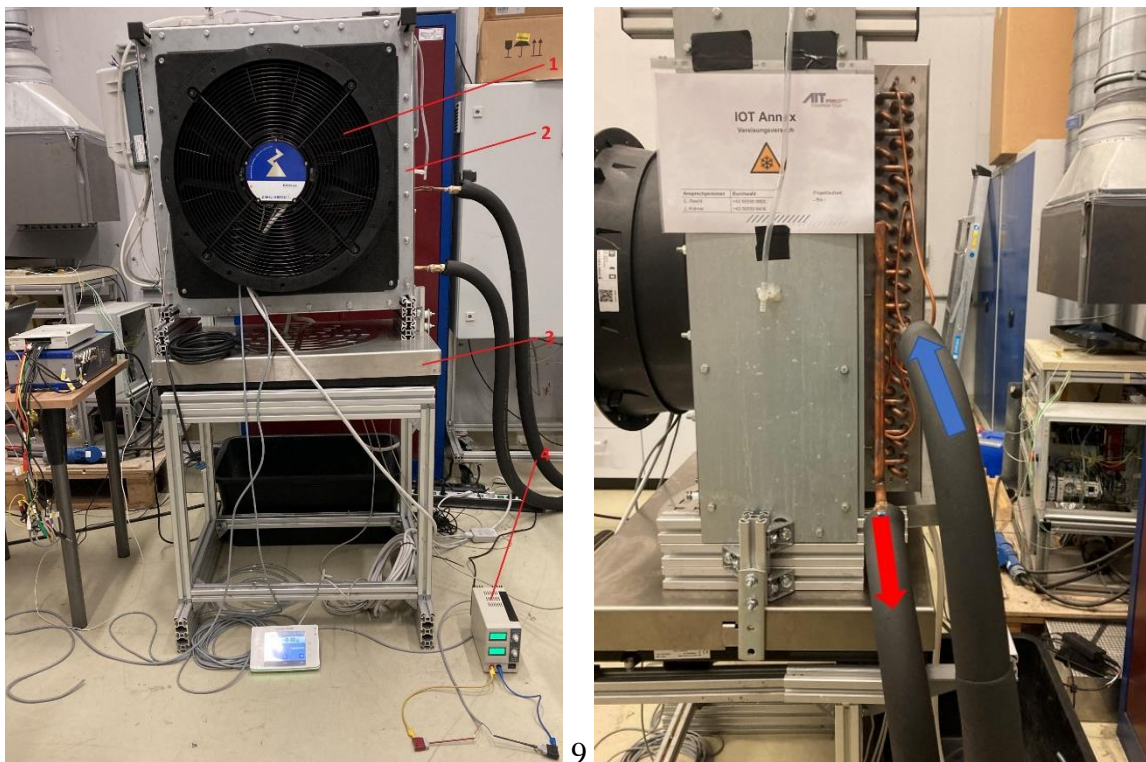


Figure 9: (left) Experimental Setup. 1: Fan, 2: dhp, 3: Scale, 4: Adjustable Power Supply; (right) side view. Upper tube carries cold water from reservoir to heat exchanger (blue arrow), lower tube carries warm water from heat exchanger back to reservoir (red arrow).

In this adapted experiment the frosting of the evaporator was performed by using a liquid with negative temperature pumped through the evaporator tubes. In that way, no compressor vibrations will be present at all. Long tubes are used for the liquid to avoid vibration influence of the external pump. The weight of the evaporator and fan vibrations signals will still be measured as in the previous setup. Image capturing and analysis is also kept as an overview concept. In addition to these data streams an external 3-axis vibration sensor is used, which can be placed on the fan casing.

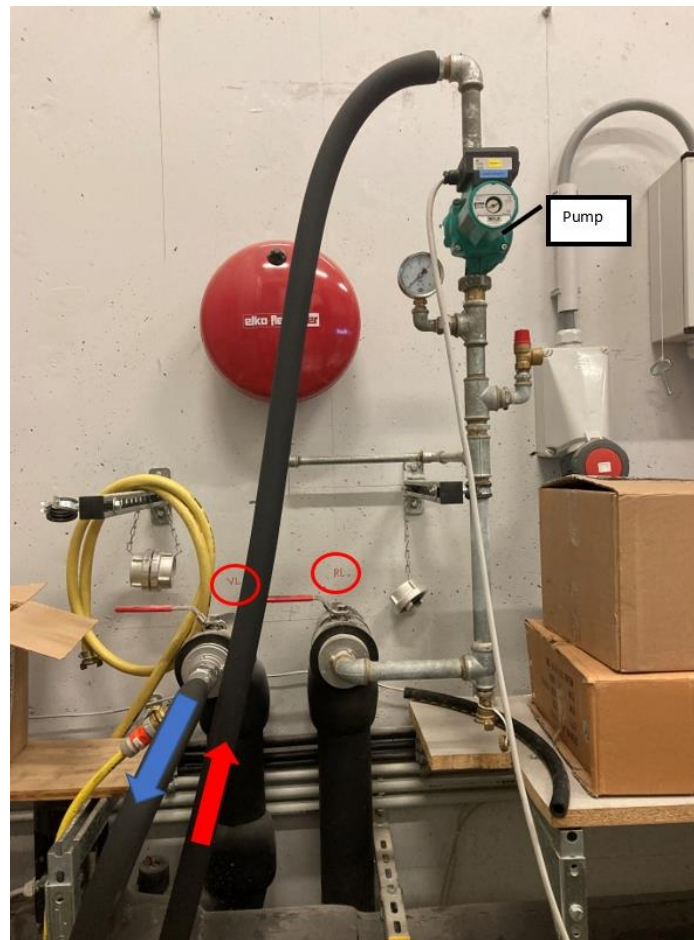


Figure 10: connection to the cold-water reservoir. VL=Vorlauf (inlet), RL=Rücklauf (outlet).

4.1. Fan Control with the Adjustable Power Supply

As stated above, the fan is controlled using an adjustable power supply. When starting the fan, usually a minimum voltage of 2V is needed to start the fan. When the fan starts spinning the voltage can also be set below 2V without issues. Increasing the voltage increases the fan speed. Currently, there is currently no other way to monitor the actual fan speed that through the ZaSet App. To install the app, the big QR-code on the side of the fan has to be scanned. Then a connection via Bluetooth to the fan entering the serial number found next to the QR-code (S/N....) and using the defined PIN is established. Once connected, the app allows for monitoring the basic operating conditions such as speed in real time. Additionally, the data coming from the fans' own sensors can be recorded using the modbus interface of the fan. Scripts have been generated to extract the fan speed and the vibration data.

4.2. Data Measurement and Collection

The main data to be collected is vibration data from the fan, the fans operational data and the weight of the frost accumulating on the heat exchanger (evaporator). For this purpose, python scripts have been generated to extract data from the three different data streams.

The first script is in charge of recording the vibrations of the vibration sensor which can be mounted freely on any metal surface (the sensor is magnetic). The sensor has 3 output channels

for the three vibration-directions. A script is also responsible for collecting data from the internal fan sensors (vibration, fan speed, power consumption, etc.) and can also be used to automatically take pictures with a webcam. The data from the fan sensors is transmitted via a cable via RS232 data link. The AIGOSS webcam is connected via USB port to the laptop.

The second script is responsible for registering the mass measured by the scale. Unlike the vibration sensor measurement, data is extracted using the RS232 data link standard.

4.3. *Vibration measurements during defrosting*

For these measurements, the setup has been modified according to Section 4.2 (also see Figure 11) for operation without evaporating refrigerant to separate heat-exchanger-fan vibration from compressor induced vibrations. Thus, the heat exchanger – fan unit was soil cooled and connected (via additional heat exchanger) to the cold water set of TechBase, AIT, Vienna. Ice accretion was accessed as in the previous setup by monitoring weight increase and image capturing and processing.

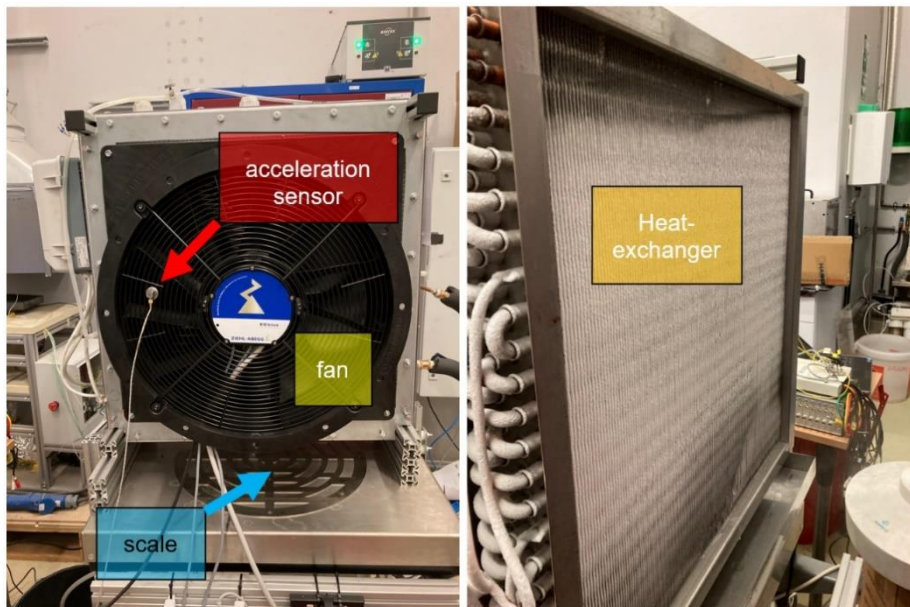


Figure 11: Modified SilentAirHP setup for soil operation: (left) fan – heat exchanger assembly on scale with mounted acceleration sensor; (right) opposite side of assembly showing the heat exchanger with ice coverage

After ice buildup, the fan was started, and the acceleration signals were monitored during subsequent defrosting (see Figure 12). After an initial increase in vibrations due to fan startup a further increase in acceleration has been observed during the progressing clearance of the air path through the heat exchanger. Thus, the decrease in vibration can be linked to the onset of defrosting possibly allowing an accelerometer being used as a soft sensor for heat exchanger frosting.

Heat Exchanger De-Icing

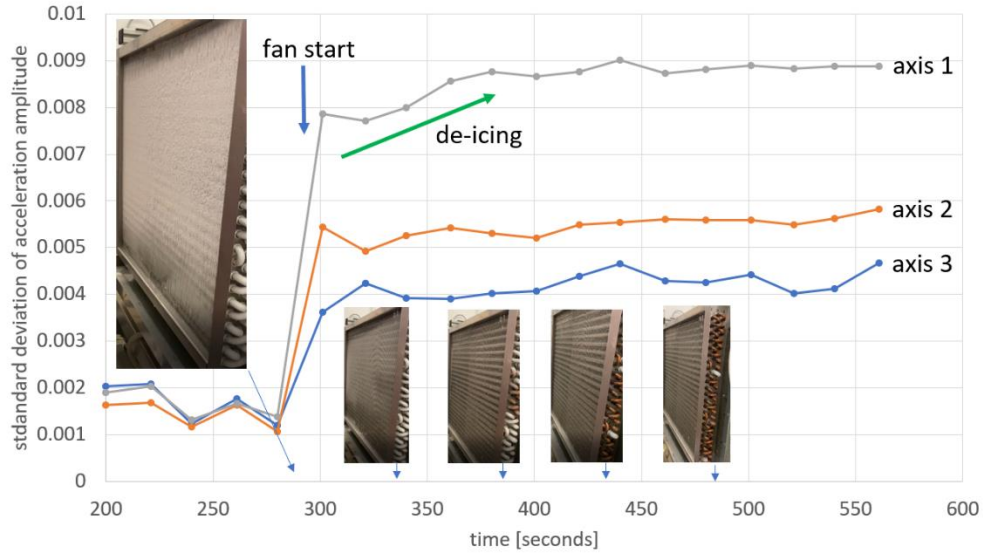


Figure 12: Increase of acceleration signals (vibration) during defrosting of the heat exchanger. The sensor has been positioned on the fan case.

4.4. Vibration measurements during artificial heat exchanger blocking

Furthermore, vibration was measured on the heat exchanger case and the fan case for various artificial heat exchanger ice coverage situations as shown in Figure 13 and 14 (the fan was switched off in the first images in both figures). Vibrations increase depending on the blockage and its symmetry breaking potential of the heat exchanger.

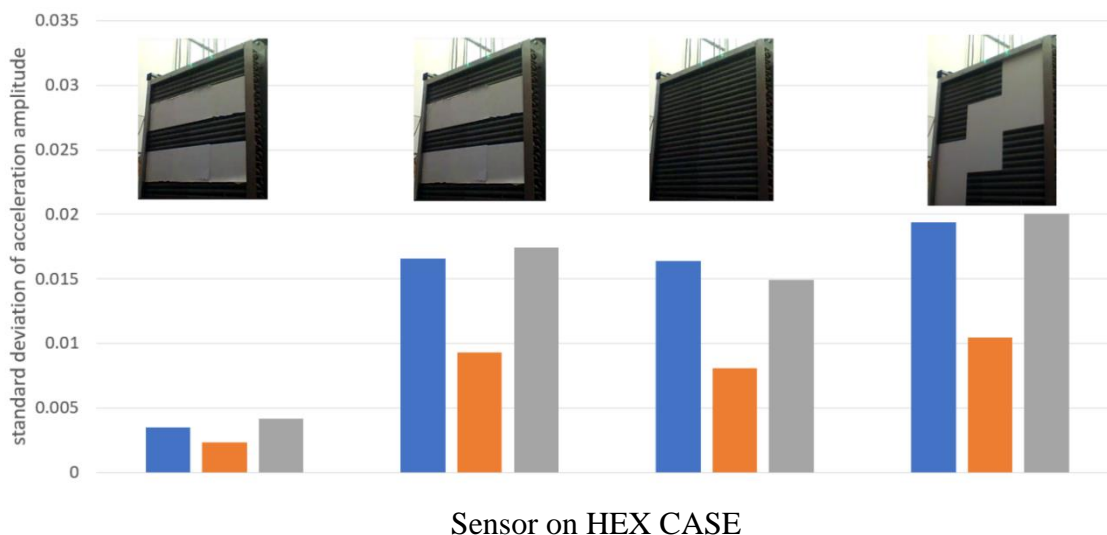
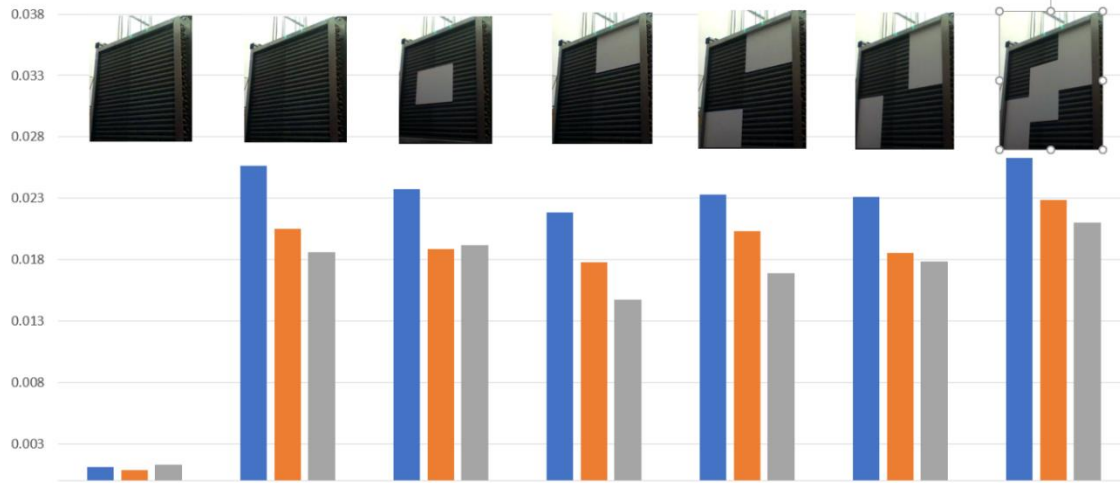


Figure 13: Acceleration measurements visualized as vertical bar charts for artificial ice coverage as shown in the images for the sensor mounted on the heat exchanger case. The first bar shows the level of vibration with the fan not operational.



Sensor on FAN CASE

Figure 14: Acceleration measurements visualized as vertical bar charts for artificial ice coverage as shown in the images for the sensor mounted on fan case. The first bar shows the level of vibration with the fan not operational.

The frequency content of the acceleration sensors depends on the mounting position of the sensor (as shown see Figure 15 for example). Therefore, the choice of sensor position will influence the capability for soft sensor ice detection usage.

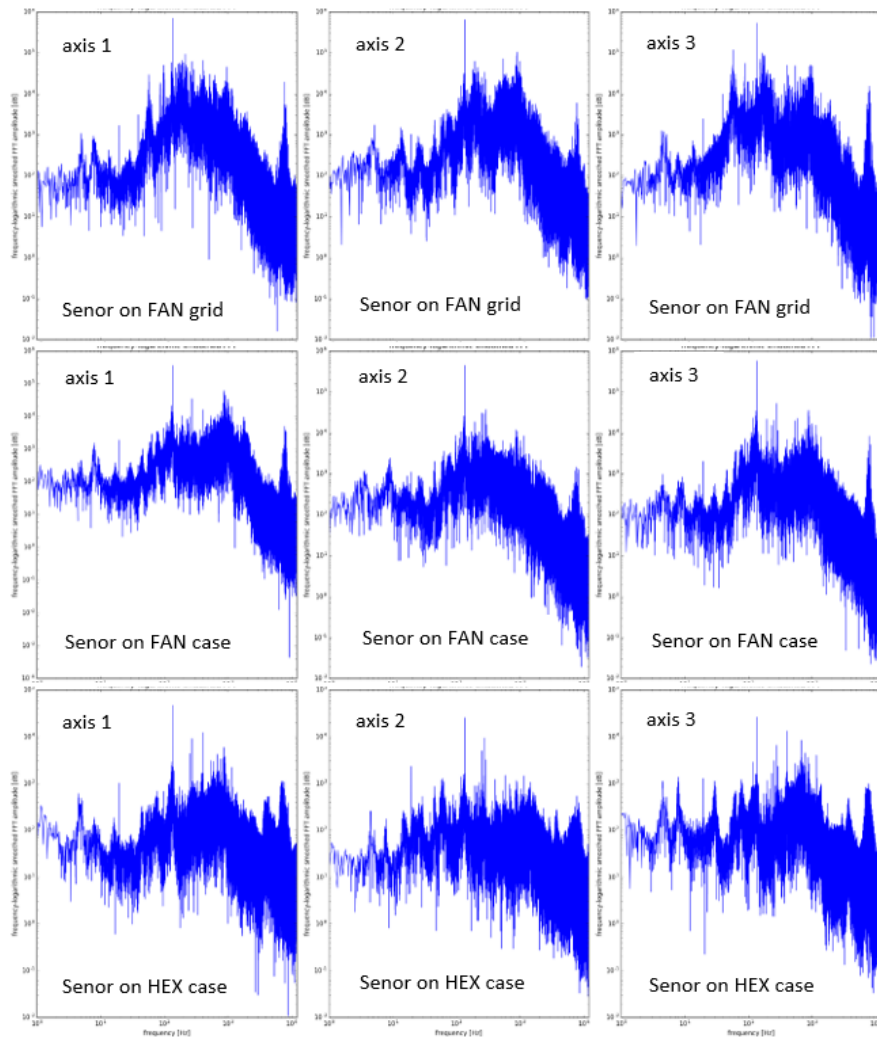


Figure 15: Frequency content of the acceleration signals depending on the mounting position of the acceleration sensor for the three recording axis. In all cases the fan was operated at fixed RPM and the heat exchanger was not covered with ice (fully free)

5. Summary

Evaporator frosting data and vibration data of a linked fan are measured simultaneously to extract a possible correlation with the final aim to use the fan-supplied vibration signals as a soft sensor for evaporator frosting. Two setups are being developed. Measurements of the first setup (SilentAirHP) have been reported showing no useable correlation due to a very low sampling frequency and bit-depth of the built-in sensor. The second setup has been built and scripts have been made available to extract the data streams of built-in vibration, power setting, evaporator weight, video camera and external vibration sensors. A change in frequency amplitude could be shown for a defrosting experiment. Using artificial heat exchanger blocking, increasing signals in the 3-axis vibration signals have been observed depending on the symmetry breaking capabilities of the heat exchanger blockage. The frequency content of these signals is dependent on the position of the sensor.



6. Acknowledgements

The Austrian Research Promotion Agency (FFG) and the Austrian Climate and Energy Fund (KLIEN) are gratefully acknowledged for funding this work under Grant No. 848891 (program line 'Energieforschung e!Mission 1st call', project 'SilentAirHP') and Grant No. 876724 (Austrian project for IEA HPT Annex 56 in the framework of the IEA Research Cooperation on behalf of the Austrian Federal Ministry for Climate Protection, Environment, Energy, Mobility, Innovation and Technology).

